A spurious-solution-free envelope function model for quantum-confined wurtzite nanostructures

Xiangyu Zhou[†*], Francesco Bertazzi[†‡], Michele Goano[†‡], Giovanni Ghione[†]
[†]Dipartimento di Elettronica e Telecomunicazioni, Politecnico di Torino,
corso Duca degli Abruzzi 24, 10129 Torino, Italy,
[‡]IEIIT-CNR, Politecnico di Torino, corso Duca degli Abruzzi 24, 10129 Torino, Italy,
[*]E-mail: xiangyu.zhou@polito.it

***Abstract*—We present a multiband envelope-function model for wurtzite nanostructures based on a rigorous numerical procedure to determine operator ordering and band parameters from nonlocal empirical pseudopotential calculations. The proposed approach leads to numerically stable envelope equations that accurately reproduce full-Brillouin-zone subband dispersions of quantum systems obtained within the linear combination of bulk bands.**

I. Introduction

Multiband $\boldsymbol{k}\cdot\boldsymbol{p}$ envelope function (EFA) models continue to play a key role in the design of III-nitride optoelectronic devices owing to their fair compromise between accuracy and computational cost. State-of-the-art GaN-based LEDs [1], [2] have complex structures thus requiring multiscale approaches to achieve a self-consistent simulation of carrier transport [3], [4], device-related effects such as current crowding, optical properties [5] and Auger transitions [5–9]. An unwelcome feature of the multiband EFA method is the appearance of spurious solutions due to incorrect operator ordering and inappropriate choices of band parameters [10], [11]. In general, $\boldsymbol{k}\cdot\boldsymbol{p}$ parameters are obtained from more fundamental calculations or experimental data through fitting procedures. Due to the lower symmetry of wurtzite crystals, which implies a larger set of parameters compared to zinc-blende semiconductors (valence band parameters A_1-A_7, crystal field splitting Δ_{cr}, spin-orbit splitting Δ_{so}, electron effective masses $m_e^{\parallel}$ and $m_e^{\perp}$, and the optical matrix parameter E_p), potential inconsistencies may arise from such fitting approaches, for different sets of parameters may produce a very similar fit to the target crystal band structure. Many strategies have been proposed to eliminate spurious solutions but none has yet found wide acceptance [12].

II. Model and method

The $\boldsymbol{k}\cdot\boldsymbol{p}$ model in our work can be considered an extension of the model proposed by Chuang [13] with amendments to account for operator ordering and nonlocal potentials. The derivation of the model is based on a nonlocal empirical pseudopotential method(NL-EPM) [14–16]. Having separated local and nonlocal components of the Hamiltonian

$$\hat{H} = \frac{\hbar^2}{2m_0}\,\nabla^2 + \hat{H}_{loc} + \hat{H}_{nl} \tag{1}$$

the relevant commutators displaying its wavevector dependence are

$$\frac{\partial \hat{H}}{\partial k} = [\hat{H}, i\hat{r}] = \frac{\hbar}{m_0}\hat{p} + [\hat{H}_{nl}, i\hat{r}] \tag{2}$$

$$\frac{1}{2}\frac{\partial^2 \hat{H}}{\partial k^2} = \frac{1}{2}[[\hat{H}, i\hat{r}], i\hat{r}] = \frac{\hbar^2}{2m_0} + \frac{1}{2}[[\hat{H}_{nl}, i\hat{r}], i\hat{r}]. \tag{3}$$

The resulting $\boldsymbol{k}\cdot\boldsymbol{p}$ Hamiltonian takes the following form

$$H_{k\cdot p} = -\frac{\hbar^2}{2m_0}\nabla^2 + \frac{\hbar}{m_0}k\cdot p + \frac{\hbar^2 k^2}{2m_0} + \hat{H}_{loc} + k\cdot[\hat{H}_{nl}, i\hat{r}] + \frac{1}{2}k^2[[\hat{H}_{nl}, i\hat{r}], i\hat{r}] \tag{4}$$

Here $\hat{H}_{loc}$ and $\hat{H}_{nl}$ are the local and nonlocal potential of the Hamiltonian, respectively. The non-commutability between potential and position operators is usually neglected in $\boldsymbol{k}\cdot\boldsymbol{p}$ theories. However, non-local potentials were found to have a significant impact on optical spectra [17]. The explicit form of the 8×8 $\boldsymbol{k}\cdot\boldsymbol{p}$ Hamiltonian including nonlocal terms is derived on the basis of quasi-degenerate perturbation theory. By replacing in the bulk Hamiltonian the wave vectors k_m with $-i\partial_m$, we obtain the finite-element discretization of the equation system for the nanostructure envelopes $F(r)$

$$\left\{-\sum_{m,n}\partial_m h^{(2)}(r)\partial_n - \sum_m\left[h_L^{(1)}(k_t,r)i\partial_m + i\partial_m h_R^{(1)}(k_t,r)\right] + h^{(0)}(k_t,r)\right\}F(r) = EF(r). \tag{5}$$

III. Simulation results

Fig. 1 compares the bulk band structure of GaN computed with NL-EPM and the present NL-EPM-derived $\boldsymbol{k}\cdot\boldsymbol{p}$ model. The valence band structure and the nonparabolicity of the conduction band are accurately reproduced near Γ. Nonlocal terms arising from the non-commutability of the Hamiltonian with the position operator were found to be critically important to reproduce the dispersion diagram. The valence subband structure of a 30 Å wide GaN/$Al_{0.2}Ga_{0.8}N$ quantum well computed with the present $\boldsymbol{k}\cdot\boldsymbol{p}$ model and NL-EPM LCBB is shown in Fig. 2. The discrepancies for higher subbands can be ascribed to the one material approximation employed in the LCBB formulation. The non-ellipticity of the EFA equations, estimated through the ρ ratio defined in Ref. [18],

978-1-4799-3682-3/14/$31.00 ©2014 IEEE

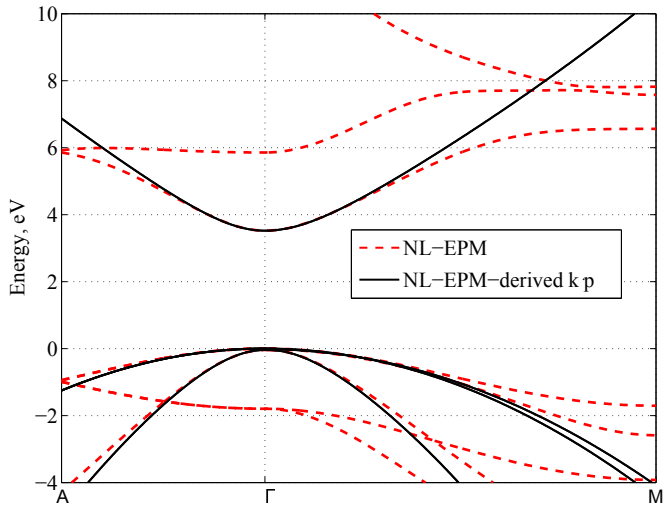

Fig. 1. Band structure of GaN, computed with NL-EPM (dashed lines) and the present $\boldsymbol{k}\cdot\boldsymbol{p}$ model with parameters derived from the corresponding NL-EPM bands (solid lines).

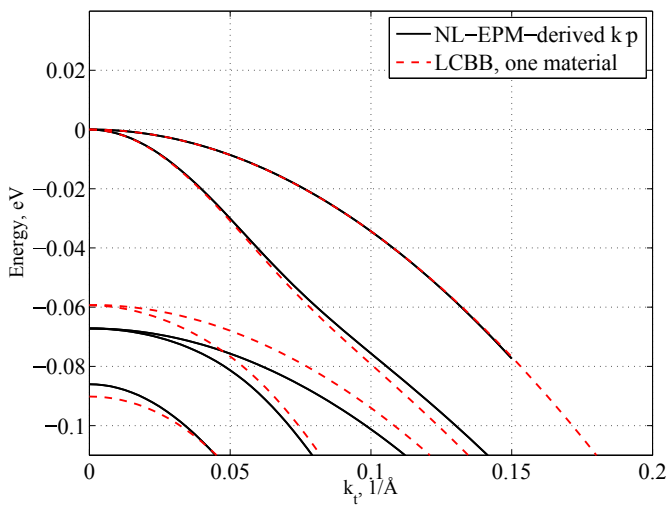

Fig. 2. Valence-subband structure of a 30 Å wide GaN/$Al_{0.2}Ga_{0.8}N$ quantum well computed with the present $\boldsymbol{k}\cdot\boldsymbol{p}$ model (solid lines), and LCBB (dashed lines).

shows a larger stability region with respect to previous $\boldsymbol{k}\cdot\boldsymbol{p}$ parametrizations, thus confirming that the proposed model is numerically stable.

IV. Conclusion

We have extended the conventional $\boldsymbol{k}\cdot\boldsymbol{p}$ theory for wurtzite crystals to account for nonlocal potentials and operator ordering. Based on a rigorous procedure to extract band parameters from nonlocal potentials, the proposed approach leads to a numerically stable finite-element model that accurately reproduces full-Brillouin-zone calculations of subband dispersions in quantum-confined nanostructures. In conclusion, the extraction procedure serves two purposes: it provides a unique set of $\boldsymbol{k}\cdot\boldsymbol{p}$ parameters and guarantees numerical stability.

References

[1] J. Cho, E. F. Schubert, and J. K. Kim, "Efficiency droop in light-emitting diodes: Challenges and countermeasures," *Laser & Photon. Rev.*, vol. 7, no. 3, pp. 408–421, Mar. 2013.

[2] G. Verzellesi, D. Saguatti, M. Meneghini, F. Bertazzi, M. Goano, G. Meneghesso, and E. Zanoni, "Efficiency droop in InGaN/GaN blue light-emitting diodes: Physical mechanisms and remedies," *J. Appl. Phys.*, vol. 114, no. 7, p. 071101, Aug. 2013.

[3] F. Bertazzi, M. Moresco, and E. Bellotti, "Theory of high field carrier transport and impact ionization in wurtzite GaN. Part I: A full band Monte Carlo model," *J. Appl. Phys.*, vol. 106, no. 6, p. 063718, Sep. 2009.

[4] F. Dolcini, R. C. Iotti, and F. Rossi, "Interplay between energy dissipation and reservoir-induced thermalization in nonequilibrium quantum nanodevices," *Phys. Rev. B*, vol. 88, no. 11, p. 115421, 2013.

[5] J. Hader, J. V. Moloney, B. Pasenow, S. W. Koch, M. Sabathil, N. Linder, and S. Lutgen, "On the importance of radiative and Auger losses in GaN-based quantum wells," *Appl. Phys. Lett.*, vol. 92, no. 26, p. 261103, 2008.

[6] F. Bertazzi, M. Goano, and E. Bellotti, "A numerical study of Auger recombination in bulk InGaN," *Appl. Phys. Lett.*, vol. 97, no. 23, p. 231118, Dec. 2010.

[7] ——, "Numerical analysis of indirect Auger transitions in InGaN," *Appl. Phys. Lett.*, vol. 101, no. 1, p. 011111, Jul. 2012.

[8] F. Bertazzi, X. Zhou, M. Goano, G. Ghione, and E. Bellotti, "Auger recombination in InGaN/GaN quantum wells. A full-Brillouin-zone study," *Appl. Phys. Lett.*, vol. 103, no. 8, p. 081106, Aug. 2013.

[9] R. Vaxenburg, E. Lifshitz, and A. L. Efros, "Suppression of Auger-stimulated efficiency droop in nitride-based light emitting diodes," *Appl. Phys. Lett.*, vol. 102, no. 3, p. 031120, 2013.

[10] M. G. Burt, "The justification for applying the effective-mass approximation to microstructures," *J. Phys. Condens. Matter*, vol. 4, no. 32, pp. 6651–6690, 1992.

[11] B. A. Foreman, "Effective-mass Hamiltonian and boundary conditions for the valence bands of semiconductor microstructures," *Phys. Rev. B*, vol. 48, no. 7, pp. 4964–4967, Aug. 1993.

[12] R. G. Veprek, S. Steiger, and B. Witzigmann, "Ellipticity and the spurious solution problem of $k \cdot p$ envelope equations," *Phys. Rev. B*, vol. 76, no. 16, p. 165320, 2007.

[13] S. L. Chuang and C. S. Chang, "$k \cdot p$ method for strained wurtzite semiconductors," *Phys. Rev. B*, vol. 54, no. 4, pp. 2491–2504, Jul. 1996.

[14] M. Goano, E. Bellotti, E. Ghillino, G. Ghione, and K. F. Brennan, "Band structure nonlocal pseudopotential calculation of the III-nitride wurtzite phase materials system. Part I. Binary compounds GaN, AlN, and InN," *J. Appl. Phys.*, vol. 88, no. 11, pp. 6467–6475, Dec. 2000.

[15] M. Goano, E. Bellotti, E. Ghillino, C. Garetto, G. Ghione, and K. F. Brennan, "Band structure nonlocal pseudopotential calculation of the III-nitride wurtzite phase materials system. Part II. Ternary alloys $Al_xGa_{1-x}N$, $In_xGa_{1-x}N$, and $Al_xIn_{1-x}N$," *J. Appl. Phys.*, vol. 88, no. 11, pp. 6476–6482, Dec. 2000.

[16] E. Bellotti, F. Bertazzi, and M. Goano, "Alloy scattering in AlGaN and InGaN: A numerical study," *J. Appl. Phys.*, vol. 101, no. 12, p. 123706, 2007.

[17] C. Motta, M. Giantomassi, M. Cazzaniga, K. Gal-Nagy, and X. Gonze, "Implementation of techniques for computing optical properties in 03 dimensions, including a real-space cutoff, in ABINIT," *Comp. Mater. Sci.*, vol. 50, no. 2, pp. 698–703, 2010.

[18] R. G. Veprek, S. Steiger, and B. Witzigmann, "Operator ordering, ellipticity and spurious solutions in $k \cdot p$ calculations of III-nitride nanostructures," *Opt. Quantum Electron.*, vol. 40, pp. 1169–1174, Jan. 2009.